The nonlinear ion-acoustic waves in a current carrying collision-dominated plasma

Autor(en): **Raemy, F. / Sayasov, Yu.S. / Schneider, H.**

Objekttyp: **Article**

Zeitschrift: **Helvetica Physica Acta**

Band (Jahr): **62 (1989)**

Heft 4

PDF erstellt am: **24.04.2024**

Persistenter Link: https://doi.org/10.5169/seals-116043

Helvetica Physica Acta, Vol. **62** (1989) 444–460 0018–0238/89/040444–17$1.50 + 0.20/0

The nonlinear ion-acoustic waves in a current carrying collision-dominated plasma

F. Raemy, Yu. S. Sayasov, H. Schneider
Department of physics, University of Fribourg, Switzerland

(10.I.1989)

Abstract: We present experiments which describe the saturation of the self-developed ion-acoustic waves in a collision-dominated current carrying plasma. The plasma with degree of ionization ranging from 30% till over 90% was generated by a capacitor discharge with maximum current-density j=20 A/cm^2 on the axis of symmetry, in a glass-tube of 20 cm diameter with a cathode-anode distance of 80 cm. The electron temperature T_e = 4.7 eV was determined by the double probe, and the ion temperature T_i = 0.7 eV by an energy analyser. The experimental results are in agreement with a nonlinear three-fluid hydrodynamical theory of ion-acoustic waves in a collision-dominated plasma, taking into account arbitrary degree of ionization, temperature oscillations and motion of neutral particles. Particularly, in agreement with this theory it was observed that the ion-acoustic instability starts in these collision-dominated plasma for electron drift velocities exceeding the ion sound velocity by an order of magnitude.The amplitude of the saturated oscillating electron density observed in our experiments as a function of the degree of ionization agrees with the theory, too.

1. Introduction

For a very long period physicists have been interested in the collective plasma phenomena. An important example of a resonant microinstability is the ion-acoustic or ion-sound instability. Ion-acoustic waves are of great interest because they can be used for the heating of a plasma [1,2]. For diagnostic purposes they serve for the determination of the plasma drift velocity [3] or of the electron temperature [4,5]. A summary of literature of the ion–acoustic waves is given by P. Michelsen [6]. Reference [7] shows a review of the theoretical and numerical work. The first measurements of the growth rate and the saturation of ion-acoustic waves, generated by optical mixing, are presented in [8]. In this reference the saturated relative density fluctuations are considered as a function of the incident power. The references [6,7,8], however, refer to collisionless plasmas.

In our experiments, performed with a current carrying argon plasma, we measured self developed ion-acoustic waves accompanied by ion-acoustic turbulence as a function of the plasma

parameters. To our knowledge we present the first measurements of the self developed saturated ion-acoustic waves in a collision-dominated plasma, and explain the saturation over a wide range of ionization degrees. The experiments presented here refer to a current carrying plasma without magnetic field.

Apart from the quasilinear theory several theories have been proposed to offer saturation mechanisms for the ion-acoustic fluctuation energy. An overview for thin plasmas is given by reference [9]. The theoretical understanding of the instability, however, is still far from satisfactory.

As a basis of our theoretical considerations of the nonlinear ion-acoustic waves and the saturation we refer to the theory of Abu-Asali, Al'terkop and Rukhadze [10,11,12] for collision-dominated plasmas and extend the theoretical analysis for a wide range of ionization degrees by taking also into account the temperature fluctuations and the motion of neutral particles.

2. Experimental set-up and basic plasma parameters

2.1 Experimental set-up

Figure 2.1 shows the experimental set-up. The plasma is generated by discharging a capacitor in a circuit with a 100 cm long tube (diameter 18.8 cm; wall thickness 6 mm) which is limited on both sides by flat stainless steel electrodes. Two crosswise arranged slots in the electrodes allow for the insertion of electric and magnetic probes in tubes of 9 mm diameter to any desired position.

During the experiment there is a steady flow of argon between anode and cathode in a pressure range of 1 to 10 mTorr. The capacitor bank, consisting of 40 parallel arranged 7.7 μF capacitors, is charged through a 80 kΩ resistance with a DC high voltage source to 6 kV. After a charge time of 50 s (τ = 25 s) the capacitor with an energy content of 5.6 kJ is sinusoidally (T/2=1.6 ms) discharged through an ignitron (GL 7703) and an inductivity (L = 0.875 mHy). The discharge current (2900 A) generates a maximum current density of 20 A/cm^2 on the major axis.

In the case of neutral gas pressures of less than 6 mTorr the described circuit fails to produce the plasma. For this reason we introduce a second discharge, this time between the third electrode and the cathode of the first described circuit. This discharge delivers enough free electrons to initiate the main discharge down to pressures of 1 mTorr.

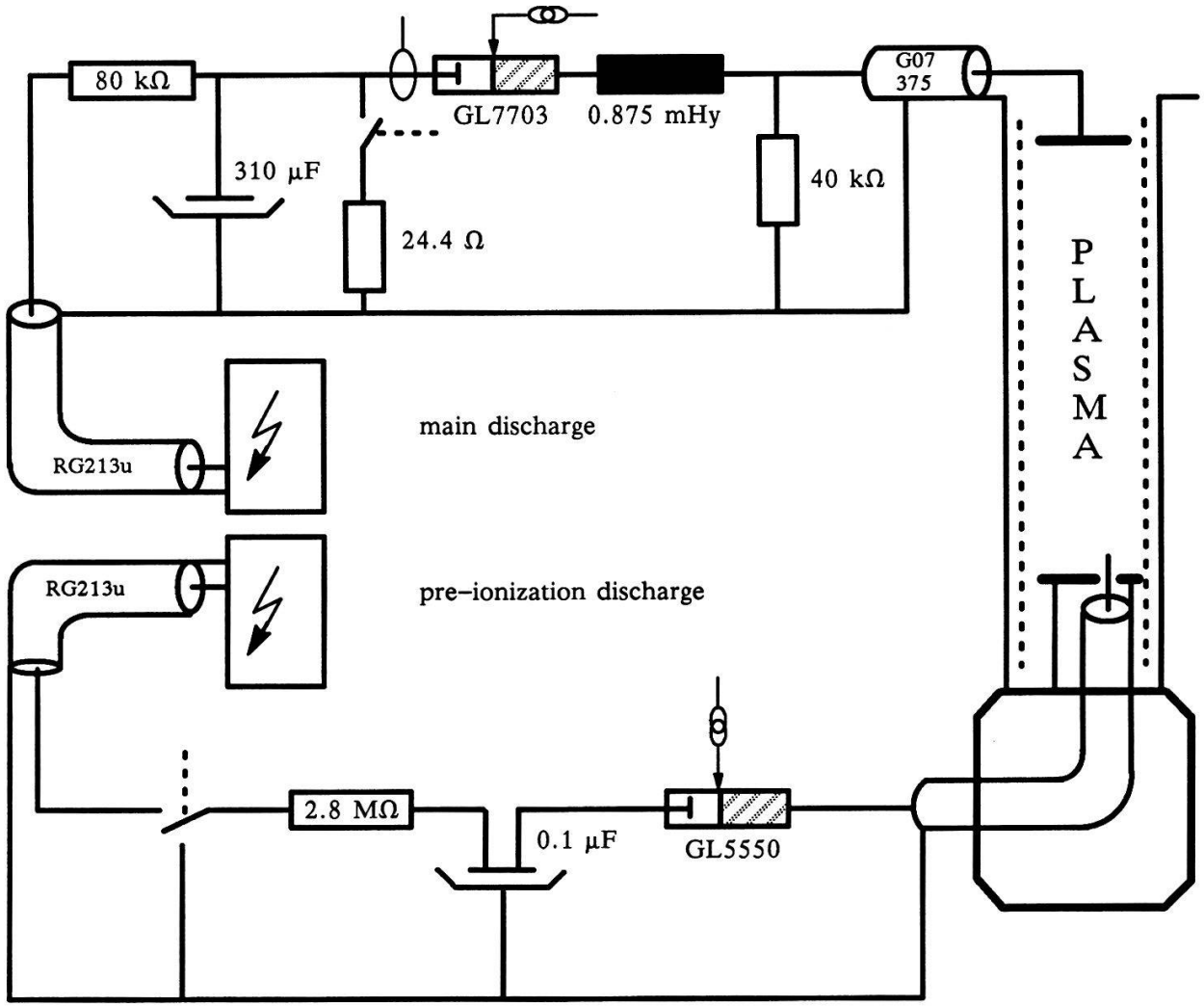

Figure 2.1 Schematic diagram of the experimental set-up

2.2 Current- and electron density measurements

According to the equations of Maxwell one finds, under the assumption of rot H » ε_0 dE/dt :

$$j(r) = 1/r\ \partial/\partial r(r\ H_\phi(r)) \qquad (2.1)$$

Figure 2.2a shows the principal arrangement of such a B_ϕ probe in the plasma. The result of a measurement of Bø as a function of radius r and time t is presented in figure 2.2b. From this three dimensional plot we derive numerically the current density according to equation 2.1, and we get the result shown in figure 2.2c.

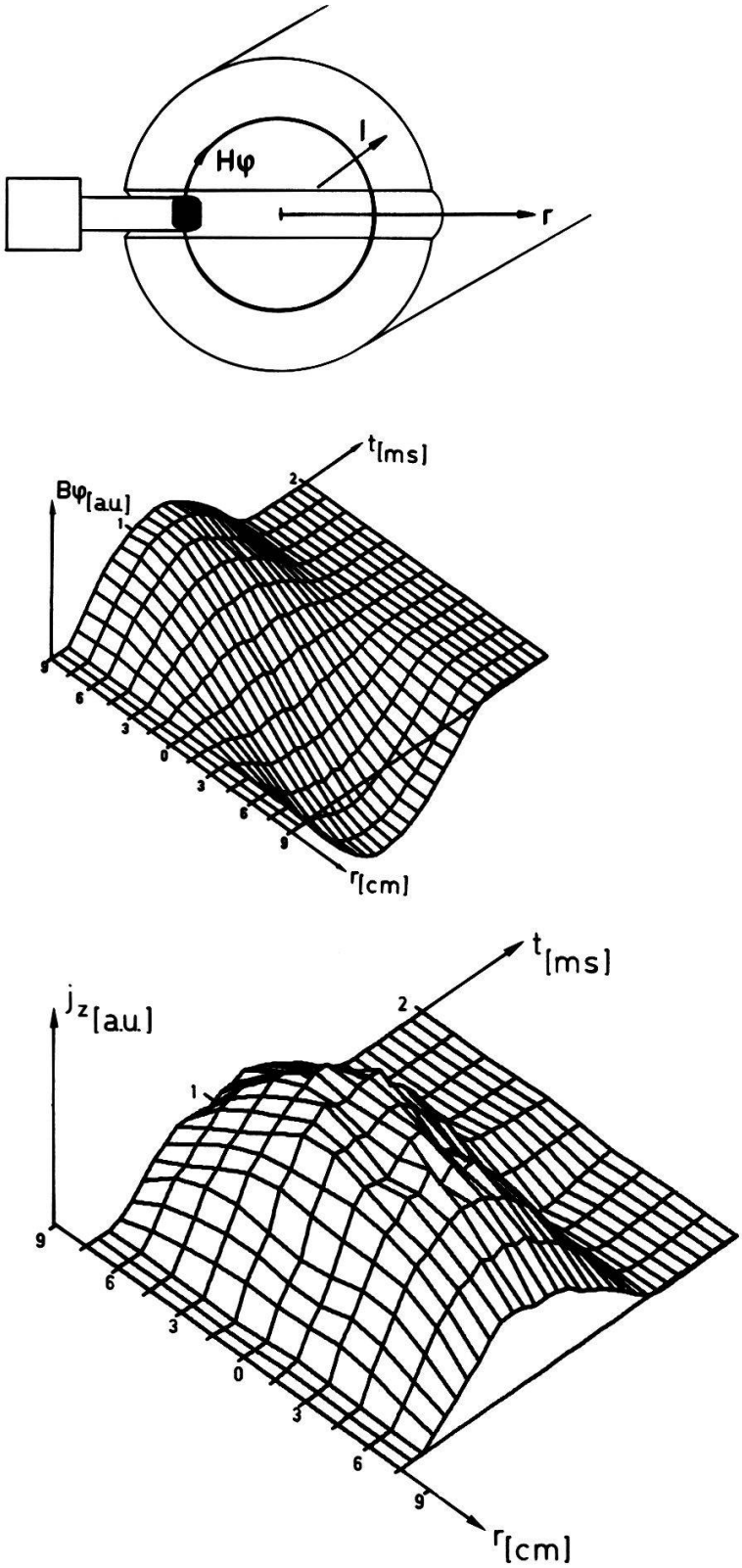

Figure 2.2 a) schematic arrangement of the B_ϕ probe
b) magnetic field $B_\phi(r,t)$
c) current density $j(r,t)$

In a further experiment we measured the electron density by means of a Langmuir double probe [13] as described in reference [14]. The results are shown in figure 3.2 where we compose the radial and time dependence of current- and electron density. The maximum value of the current density is 20 A/cm^2 and the electron density has been found to be 6.3 10^{13} cm^{-3}.

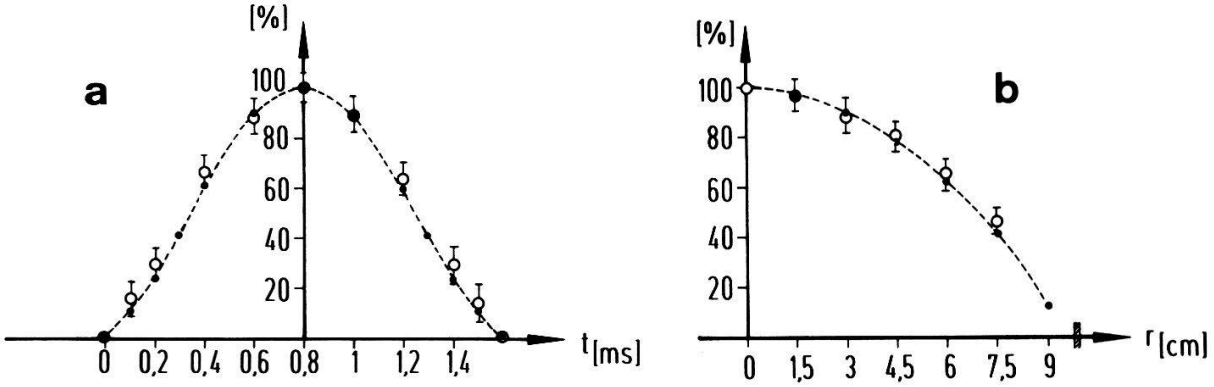

Figure 2.3 a) .... measured particle density $n_e(t)/n_e(t_{max})$
oooo measured current density $j(t)/j(t_{max})$
b) .... measured particle density $n_e(r)/n_e(r=0)$
oooo measured current density $j(r)/j(r=0)$

From this accordance in the radial and time dependent profile of the current density and electron density we obtain an important result: The drift velocity of the electrons v_d = constant as a consequence of $j \sim n_e$. Other plasma parameters are listed in table 1 below.

discharge tube:	length 1m
	diameter 18.8 cm
	plasma length 80 cm
plasma parameters:	discharge current 2900A
	current density 20 A/m^2
	electron temperature 5 eV
	ion temperature 0.8 eV
	electron density 6.3 10^{19} m^{-3}
	v_d electron drift velocity 2.10^4 m/s
	ν_{ei} electron-ion collision frequency
	ν_{ii} ion-ion collision frequency
	$\nu_{ia}=10^{-9}n_a$ [1/s] electron-atom collision frequency (according to [9])
ion-acoustic wave:	frequency 24 kHz
	wavelength 16 cm
	phase velocity 3.4 10^3m/s

Table 1 Parameters

3. Experimental investigation of the nonlinear ion-acoustic waves

For the current density (j=20 A/cm^2) and the electron density n_e=6.3 10^{13} cm^{-3} and a mean electron temperature T_e = 4.7 eV it turns out that the drift velocity of the electrons exceeds the ion sound velocity by several times. Under this conditions we expect the appearance of ion-acoustic waves in the plasma.

3.1 Experimental set-up

Figure 3.1 shows the electronic diagram which consists of two double probes measuring the electron density. Instead of a transformer [14] we use two current probes (A 6302) with two current to voltage converters (AM 503) to protect the A/D oscilloscope (LC 9400) from primary discharge high voltage.

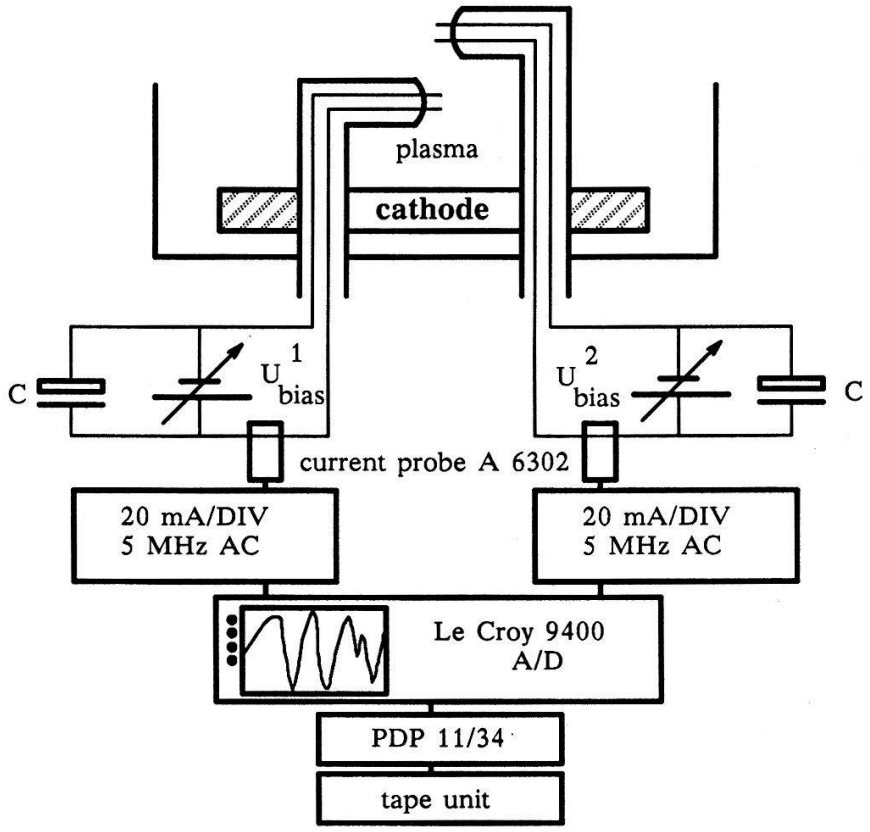

Figure 3.1 Two double probe arrangement in the discharge tube

The time dependent signals of figure 3.2 show that the mean electron density does not change, but with increasing ionization degree the fluctuations become significant. In the high ionization case we investigate the fluctuations by the digital spectral analysis applying ZOOM-FFT technique

[15,16]. The key idea underlying the wave and instability identification is to compute auto- and cross-power spectral density functions using FFT techniques in order to determine frequency, wavelength and phase velocity.

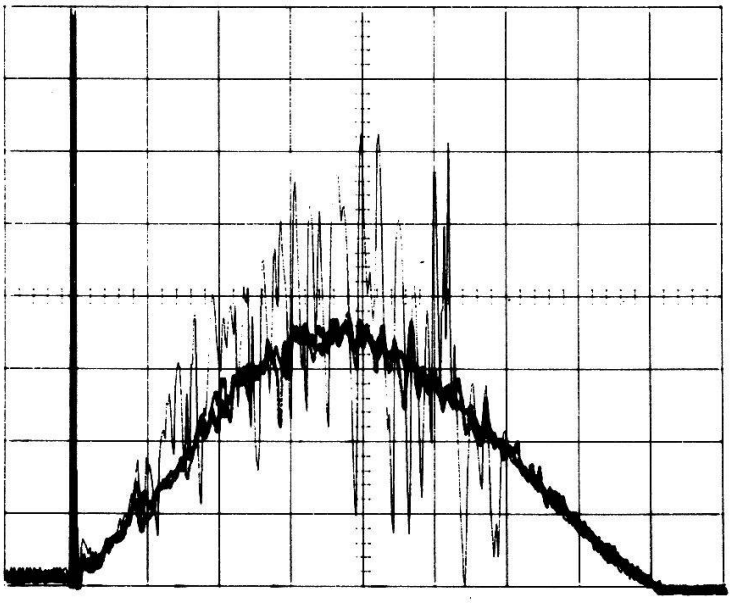

Figure 3.2 Time dependent density fluctuations for different ionization degrees; 0.2ms/div

3.2 Spectrum of density fluctuations and identification of the wave

Figure 3.3 gives the typical auto power spectrum with a main peak at the frequency f=24 kHz in argon at a neutral gas pressure p = 2.4 mTorr.

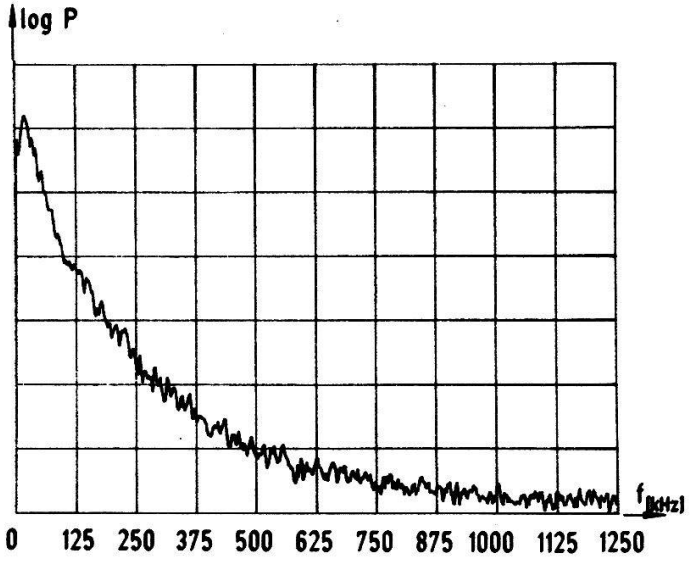

Figure 3.3 Auto-power spectrum
log p [a.u] versus frequency in kHz at p=2.4 mTorr argon

Noticing the phase difference as a function of the distance for the main peak (fig.3.3) between the two double probes on the major axis x, we find the propagation velocity of the wave (from fig.3.4) $v_\phi = 3.4\ 10^5$ cm/s and the corresponding wavelength $\lambda = 14$ cm ($k = 2\pi/\lambda = 0.44\ cm^{-1}$).

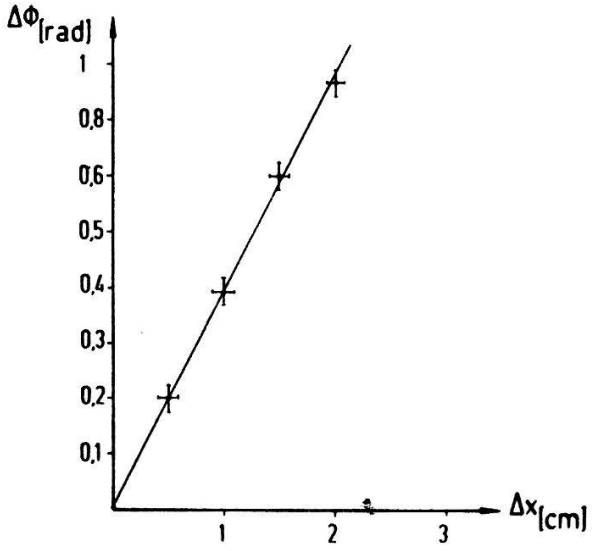

Figure 3.4 Phase difference as a function of the distance between the two probes for f=24 kHz and pressure p = 2.4 mTorr

From the phase spectrum (fig 3.5) follows the dispersion relation found by the phase measurement of the two probes in a distance $\Delta x = 1$ cm. In the low frequency part of the spectrum (with the coherence 1) the phase is proportional to the frequency. As a consequence of this, the dispersion relation is a linear function and the wave is propagating with constant phase velocity along the x axis according to figure 3.1. A comparison of the phase velocity with the ion-sound velocity ($v_S = (T_e/m_i)^{1/2} = 3.35\ 10^5$ cm/s; m_i is the ion mass) confirms the identification of ion-acoustic waves.

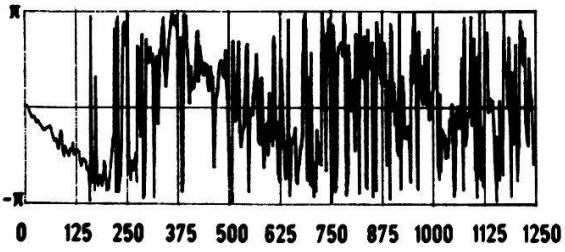

Figure 3.5 Phase-spectrum of the two double probes in a distance of 1 cm on the plasma axis ($\Delta\phi$[rad] versus frequency [kHz])

From figure 3.5 we derive a linear relationship between the wavenumber k and the frequency ω for the low frequency part of the spectrum. This will be discussed in the next part of this paper.

4. Theory of nonlinear ion-acoustic oscillations in collision-dominated plasmas

The plasmas investigated in these experiments can be considered as collision-dominated in the sense that the collision frequencies ν_e, ν_i are big enough, i.e. the electron and ion mean free paths are much smaller than the wave-length $\lambda = 2\pi/k$ of the ion-acoustic oscillations excited in the plasma. Under these conditions stabilization of the ion-acoustic waves occurs mainly as a result of collisions of plasma ions with plasma particles, in contrast with thin plasmas in which the stabilization occurs as a result of the ion Landau-damping. A theory of nonlinear ion-acoustic oscillations in two-fluid approximation was developed in [10,11,12] for two limiting cases - for weakly ionized plasmas where only electron and ion-neutral collisions are of importance, and, on the other hand, for strongly ionized plasmas where only collisions between charged particles are of importance.

In the present experiments, performed in broad diapason of electron concentration, collisions of all types must be considered simultaneously. In addition, the level of saturated electron density oscillations can be high. Moreover, for the observed oscillation frequencies ω comparable with the ion collision frequency ν_i the two-fluid approximation may not be valid i.e. the motion of the neutral gas must be accounted for as well. In the following, the theory described in [10,11,12] is generalized to meet the realistic conditions existing in this experiment.

As in [10,11] it will be assumed that the problem is a one-dimensional one, i.e. that all quantities depend on the coordinate x counted along the plasma axis only. The basic equations of three-fluid hydrodynamics for non-isothermal plasma ($T_i \ll T_e$), under the the assumption of quasi-neutrality ($n_i=n_e=n$) and the neglection of electron inertia, can be formulated as follows:

$$m_i n\left(\frac{\partial v_i}{\partial t} + v_i \frac{\partial v_i}{\partial x}\right) = -\nabla(T_e n) - m_i n \nu_{ia}(v_i - v_a) + m_i X_i n \frac{\partial^2 v_i}{\partial x^2} \tag{4.1}$$

$$m_i n_a\left(\frac{\partial v_a}{\partial t} + v_a \frac{\partial v_a}{\partial x}\right) = m_i n \nu_{ia}(v_i - v_a) + m_i X_a n_a \frac{\partial^2 v_a}{\partial x^2} \tag{4.2}$$

$$\frac{\partial n}{\partial t} + v_i \frac{\partial n}{\partial x} + n \frac{\partial v_i}{\partial x} = 0 \tag{4.3}$$

$$\frac{\partial n}{\partial t} + (v_d + v_e)\frac{\partial n}{\partial x} + n \frac{\partial v_e}{\partial x} = 0 \tag{4.4}$$

$$n T_e\left(\frac{\partial S}{\partial t} + (v_d + v_e)\frac{\partial S}{\partial x}\right) = \frac{\partial}{\partial x}\left(n X \frac{\partial T_e}{\partial x}\right) \tag{4.5}$$

Here v_i, v_e, v_a are respectively the ion, electron and neutral particle velocities, $v_d = eE/m_e\nu_e$ is the electron drift velocity, $S=\ln(T_e/n^{\gamma-1})$, $\gamma = 5/3$. The coefficient m_iX_i is the ion viscosity which is under the present conditions mainly due to the ion-ion collisions, i.e. $X_i=1.28\ T_i/m_i\nu_{ii}$ (ν_{ii} being the ion-ion collision frequency), $X_a = T/m_i\nu_{ia}$ is the neutral particle viscosity. The coefficient X is the electron thermal conductivity, which according to the mixture rule, can be represented by

$$\frac{1}{X} = \frac{1}{X_{ei}} + \frac{1}{X_{ea}}$$

with $X_{ei}=3.16T_e/(m_e\nu_{ei})$ and $X_{ea}=T_e/(m_e\nu_{ea})$. Note that in general the electron collision frequencies ν_{ei}, ν_{ea} entering X and v_d can include the turbulent effects, and thus differ essentially from classical values. Using the assumption [10,11] that the saturated ion-acoustic wave is a function of the argument $\xi=kx-\omega t$ only, we can reduce the system (4.1)-(4.5) to a set of ordinary differential equations:

$$-w'(1-w) = -\beta^2(\tau'-\rho') - \frac{\nu_i}{\omega}(w-w_a) + \gamma_i w'' \qquad (4.1')$$

$$-w'_a(1-w_a) = g(w-w_a) + \gamma_a w''_a \qquad (4.2')$$

$$-\rho'(1-w) + w' = 0 \qquad (4.3')$$

$$\rho'(\alpha - 1 + w_e) + w'_e = 0 \qquad (4.4')$$

$$\tau'' + w'\tau' = -\delta(1 + \frac{w_e}{\alpha-1})(w' - \tfrac{2}{3}\tau') \qquad (4.5')$$

Here $\rho = \ln(n/n_o)$, $w=\kappa v_i/\omega$, $w_e = kv_e/\omega$, $w_a=kv_a/\omega$, $g=\nu_i n/(\omega n_a)$, $\delta=\omega(\alpha-1/(Xk^2))=\mu\nu_{eff}(\alpha-1)/\omega$, $\alpha=v_dk/\omega$, $\nu_{eff}=(\nu_{ei}/3.16)+\nu_{ea}$, $\gamma_i=X_ik^2/\omega$, $\gamma_a=X_ak^2/\omega$, $\tau=T_e/T_{eo}$, T_{eo}, n_o are the undisturbed electron temperature and density. Prime means differentiation with respect to ξ, $\beta=v_Sk/\omega$, $v_S=(T_e/m_i)^{1/2}$. As follows from (4.3'), $\rho = \ln(1+n'/n_o)=-\ln(1-w)$ i.e.

$$\frac{n'}{n_o} = \frac{w}{1-w} \qquad (4.6)$$

where n' is the fluctuating part of the electron density ($n=n_o+n'$). Assuming $\delta \ll 1$ we can reduce the equation (4.5') to $\tau'' = -\delta w'$,i.e. $\tau' = -\delta w$ Assuming also $g \ll 1$ we can take $w_a \ll w$ i.g. to neglect w_a in (4.1'). Inserting $\tau' = -\delta w$ and $\rho'=w'/(1-w) \approx w'(1+w)$ into (4.1') we can reduce it to

$$\gamma_i w'' - 2ww' + (1-\beta^2)w' + \Gamma w = 0, \quad \Gamma = \delta - \frac{\nu_i}{\omega} \tag{4.7}$$

In this form (4.7) coincides with eq. 4.1 in [10] (for slightly ionized plasmas) where $\nu_{ea} \gg \nu_{ei}/3.16$, or for $\nu_{ea} \ll \nu_{ei}/3.16$ with eq. 11 in [11] (for strongly ionized plasmas). As it was shown in [10,11] the equation (4.7) allows a periodic solution, having a period of 2π ($w(0)=w(2\pi)=0$), corresponding to saturated ion-acoustic waves, in case $\beta=1$ i.e. the dispersion relation

$$\omega = v_S k \tag{4.8}$$

which is characteristic for the linear ion-acoustic wave must be also valid for nonlinear saturated waves described by the equation (4.7). According to [10,11], the periodic solution of (4.7) can be represented explicitly by the formula

$$w = \frac{\Gamma}{\sqrt{2(\varepsilon+1}}\frac{dh}{d\tau} \quad , \quad \tau = \sqrt{2(\varepsilon+1)}\,\xi, \quad \varepsilon = \frac{\Gamma}{\gamma_i} - 1 \tag{4.9}$$

where h is the function satisfying the equation

$$2\frac{d^2h}{d\tau^2} - \left(\frac{dh}{d\tau}\right)^2 + h = 0 \tag{4.10}$$

It allows the first integral

$$\left(\frac{dh}{d\tau}\right)^2 = F(h) = Ce^h + h + 1, \quad C < 1$$

i.e. the function $h=h(\tau)$ can be defined by the relation

$$\int_{h_o}^{h} \frac{dh}{\sqrt{F}} = \tau = \sqrt{2(\varepsilon+1)}\,\xi \tag{4.11}$$

The condition of periodicity of $h=h(\xi)$ provides the relation

$$\int_{h_o}^{h_1} \frac{dh}{\sqrt{F}} = \sqrt{2(\varepsilon+1)}\pi,\ F(h_{0,1}) = 0 \tag{4.12}$$

defining the constant of integration $C = C(\varepsilon)$. This constant can be expressed for the two limiting cases $\varepsilon \to 0$ and $\varepsilon \to \infty$ by the asymptotic formulas

$$C = 1 - \varepsilon\ ,\quad \varepsilon \to 0$$
$$C = \exp\left(-\frac{\pi^2(\varepsilon+1)}{2}\right),\quad \varepsilon \to \infty \tag{4.13}$$

For intermediate values of ε the constant $C=C(\varepsilon)$ was obtained by numerical integration of (4.12). It is given in Fig. 4.1.

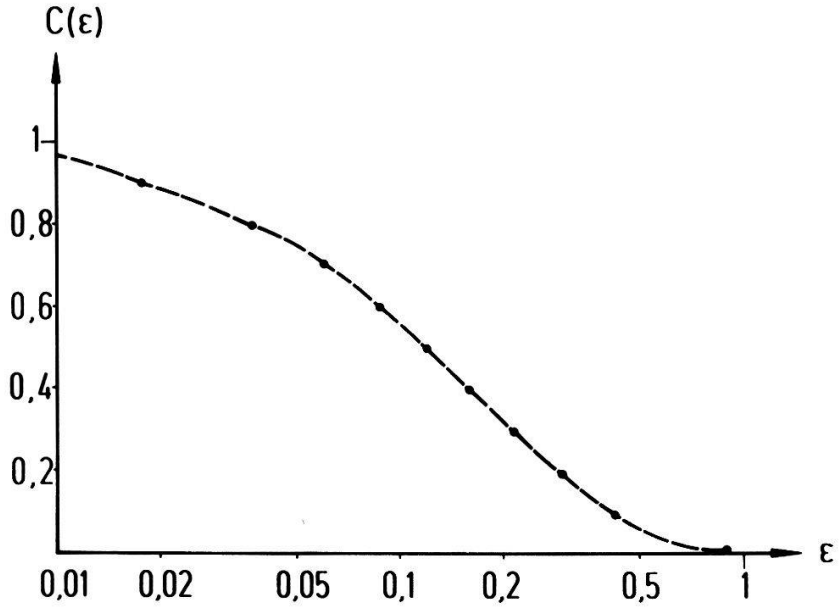

Figure 4.1 $C(\varepsilon)$, $0.01 < \varepsilon < 1$.

The maximum value of the density fluctuation $(n'/n_o)=w_{max}$ can be now found by the formula

$$\left(\frac{n'}{n_o}\right)_{max} = \tfrac{1}{2}\Gamma f(\varepsilon),\ f(\varepsilon) = \sqrt{\frac{2}{(\varepsilon+1)}\ln\frac{1}{C}}\ . \tag{4.14}$$

The function $f(\varepsilon)$ is given in Fig. 4.2.

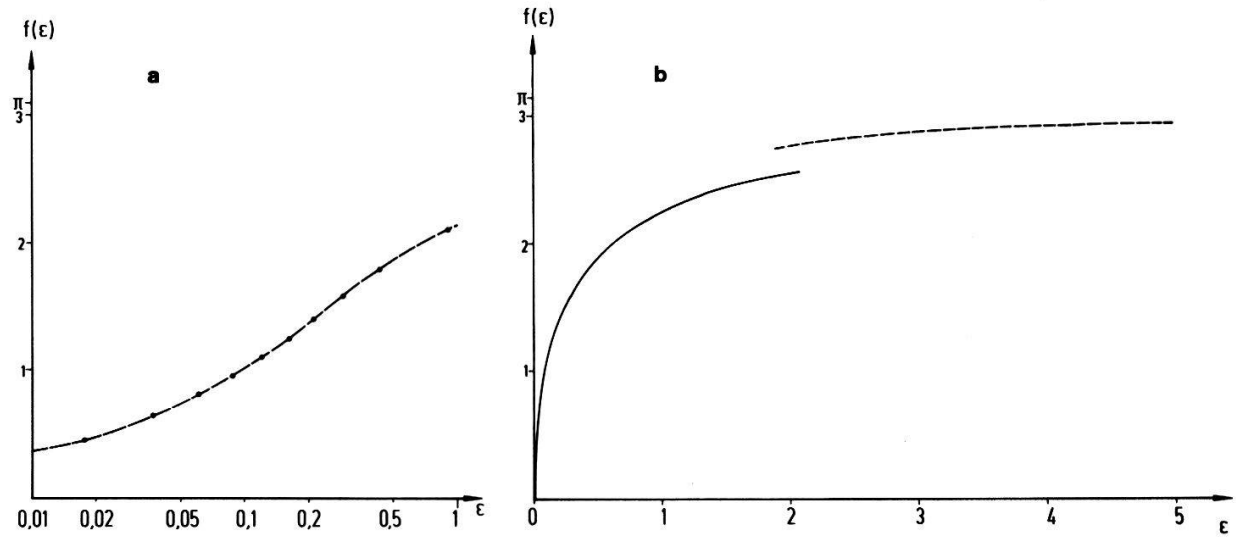

Figure 4.2 a) $f(\varepsilon)$, $0.01 < \varepsilon < 1$

b) $f(\varepsilon)$ in the limits according to (4.13). The dotted line corresponds to the formula (4.13) in reference [10].

The experimental conditions correspond to the assumption $\varepsilon >> 1$. In this case $f(\varepsilon) = \pi$ i.e. $(n'/n_o)_{max} = \pi\Gamma/2$. This formula can be found also from elementary considerations. For $\varepsilon >> 1$ we neglect the term $\gamma_i w''$ in (4.7) thus obtaining the solution $w = \xi\Gamma/2$. The real solution represents in fact a sawtoothed curve (Figure 4.3). However the linear solution $w=\xi\Gamma/2$ holds almost in the whole interval $0 \leq \xi < \pi$ and breaks down only in a very narrow interval adjoining $\xi \leq \pi$, decaying very quickly to $w=0$ for $\xi \to \pi$. Thus, to obtain w_{max} we can simply put $\xi=\pi$ in $w=\xi\Gamma/2$, getting $w_{max} = \Gamma\pi/2$. (A more detailed analysis shows that this simple approach involves errors of the order of $\varepsilon^{-1/2}$). In the conditions of our experiment $\varepsilon \approx 10^3$. Thus this approximation is very good. For the parameters summarized in table 1 we get

$$\left(\frac{n'}{n_o}\right)_{max} = w_{max} = \frac{\pi}{2} \cdot 0.5\left(1 - 0.5\frac{1-x}{x}\right) \quad (4.15)$$

This formula provides already a reasonable description of experimental curve representing the density fluctuation n'/n_o as a function of the degree of ionization (curve b_1 in Fig.5.1).

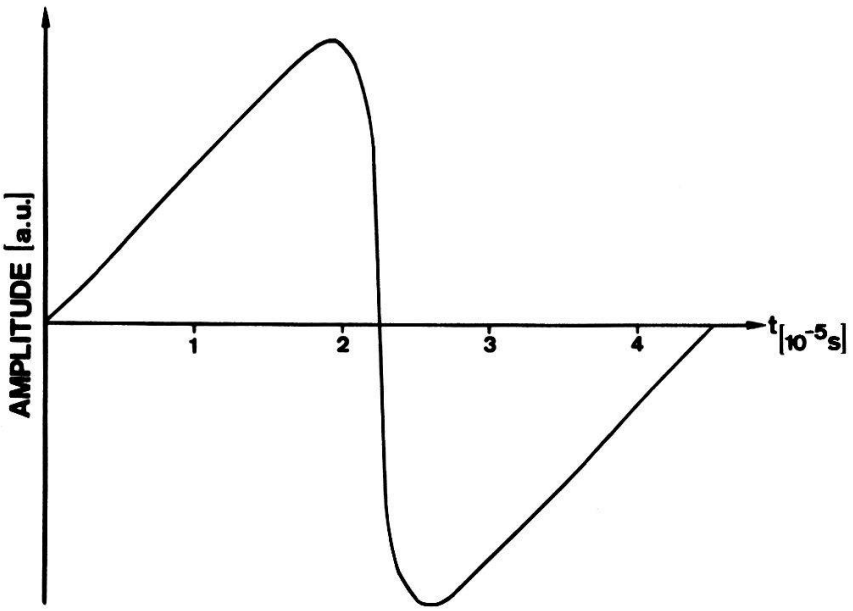

Figure 4.3 Solution w(kx - ωt) for one period

A better description of the experiment can be achieved by considering effects due to the motion of the neutral particles. These effects must be especially pronounced for the high degree of ionization when the parameter $g=\nu_i n/(\omega n_a)$ becomes large. Qualitatively, this corresponds to the fact that at high degree of ionization the neutral particles get involved in the oscillatory motion and, hence, the relative velocity v_i-v_a becomes small. Accordingly, the friction force $m_i\nu_i n(v_i-v_a)$ experienced by the ions drops essentially. In the approximation $w_a \sim \Gamma$ these effects can be described by considering instead of (5.7) the set of equations

$$\gamma_i w'' - 2ww' + \delta w - \frac{\nu_i}{\omega}(w - w_a) = 0$$
$$-w'_a = g(w - w_a) \qquad (4.16)$$

(We drop here the small term $\gamma_e w''$ and $(\beta^2-1)w'$). A tentative estimate of the maximal value of $w \approx n'/n_o$ defined by (4.16) can be done by the collocation method [17]. We will use the trial functions

$$w = A\xi, \quad w_a = Bg(\pi^2 - \xi^2)$$

where A,B are some constants. Inserting them into (4.16) and neglecting the term $\gamma_i w''$ we get the residual equation

$$R(\xi_o) = \frac{\nu_i}{2\omega} \cdot \frac{Ag(\pi^2 - \xi_o^2) / \xi_o}{1 - g(\pi^2 - \xi_0^2) / 2\xi_o} - (2A^2 - \Gamma A) = 0$$

which defines the constant A by the requirement of $R(\xi_O)=0$ for a choosen point $\xi=\xi_O$. Assuming $\xi_O=\pi/2$ we get

$$A = \frac{1}{2}\left(\delta - \frac{\nu_i}{\omega} \cdot \frac{1}{1 + \frac{3\pi}{4}g}\right)$$

and hence

$$\left(\frac{n'}{n_0}\right)_{max} = w_{max} = A\pi = \frac{\pi}{2} \cdot 0.5\left(1 - 0.5\frac{(1-x)/x}{1 + 0.8\frac{x}{1-x}}\right) \qquad (4.17)$$

This approach corresponds to the introduction of a modified ion-neutral collision frequency $\nu_{eff}=\nu_i/(1+g3\pi/4)$ taking into account the reduction of friction force for high degree of ionization. The curve b_2 in Fig. 5.1 gives a better agreement with the experimental result. The analysis based on the formulas (4.15) and (4.17) is certainly not complete since the parameter Γ is in fact not so small. However, in virtue of theorems in [18], asserting that the solution $w=w(\xi)$ as given by (4.1')-(4.5') can not differ essentially from the solution of (4.7) if the parameter Γ is not too large, one can state that the qualitative features of the nonlinear ion-acoustic oscillations are represented correctly by these formulas.

5. Results and discussion

5.1 The saturation of nonlinear ion-acoustic oscillations as a function of ionization degree

The most important result of our investigation is the demonstration of the saturation of ion-acoustic waves as a function of ionization degree. The nonlinearity of the present ion-acoustic instability manifests itself in the way, that the amplitude of the fluctuation after a very short time compared with the discharge time reaches a state of saturation. This has been observed over a wide range of ionization degrees.

From the digital data n_{ei} (i=1,...,N), determining the standard deviation, and relating the result to the mean density we have

$$\frac{n'_e}{\bar{n}_e} = \frac{1}{\bar{n}_e}\left(\frac{1}{N-1}\sum_{i=1}^{N}(n_{ei}-\bar{n}_e)^2\right)^{\frac{1}{2}} \tag{5.1}$$

which is the relative saturated density fluctuation.

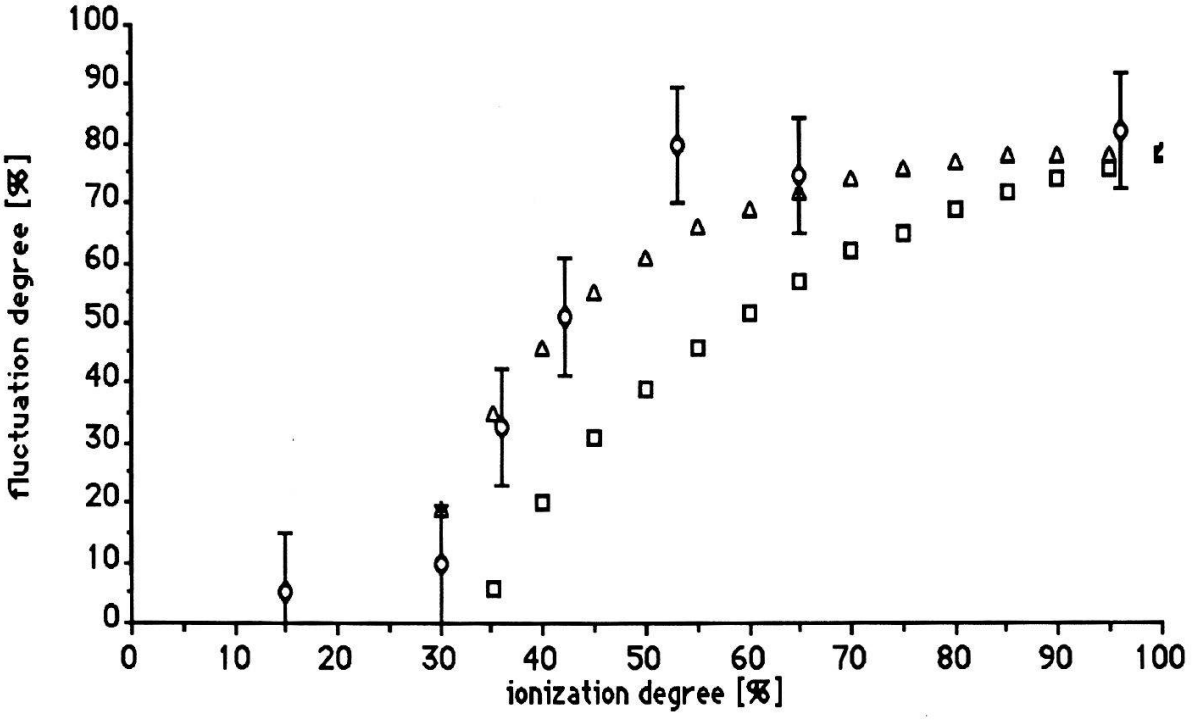

Figure 5.1 Saturated relative density as a function of the ionization degree with $\nu_{e,eff}=16\nu_{ei}$
a) experimental o b1) theoretical (as formula 4.15) □
b2) theoretical (as formula 4.17) Δ

The results of the relative saturated density fluctuations, whitch we identified as ion-acoustic waves, represented as a function of the ionization degree (fig 5.1) are compared with our theoretical considerations of chapter 4. Whereas in the range of low ionization degrees the amplitude of the ion-acoustic wave is almost 0%, in the high ionization region there appear saturated amplitudes of about 80% related to the mean electron density. The transition is located between 30% and 50% of ionization degree. The curve b_1 in figure 5.1 shows the result of the expression 4.15 based on the theoretical investigations of reference [10,11,12], b_2 represents the extended theoretical consideration which confirms the sensitivity of the saturation level on effects due to the motion of the neutral particles (4.17).

5.2 Conclusion

To our knowledge we present the first experimental results showing the saturation level of self developed ion-acoustic waves over a wide range of ionization degrees in a collision-dominated plasma.

The main result which confirms our interpretation of experiments in terms of nonlinear ion-acoustic waves can be summarized as follows:

From the experimental results showing that the current-density is proportional to the density of charged particles and that v_d widely exceeds v_s, which is characteristic for collision-dominated plasmas, it can be concluded that the electron drift velocity during this slow experiment is constant and therefore we are dealing with ion-acoustic waves.

The linear dispersion relation (4.8) holds also for the nonlinear ion-acoustic waves.

Despite of many simplifications our theoretical description of the saturation mechanism fits well with the experiment (Fig. 5.1).

References

[1] C. Wharton, P. Korn, D. Prono, S. Robertson, P. Auer and C.T. Dum, in Proceedings of the 4th International Conference on Plasma Physics and Controlled Nuclear Fusion Research, Madison, 1971 (IAEA, Vienna, 1972), Vol.II, p. 25-37.
[2] S.M. Hamberger, UI. Jancarik, L.E. Sharp, D.A. Aldcroft and A. Wetherell, in Proceedings of the 4th International Conference on Plasma Physics and Controlled Nuclear Fusion Research, Madison, 1971 (IAEA, Vienna 1972), Vol.II p.37-53.
[3] H. Hsuan, M. Okabayashi and S. EJIMA, Nucl. Fusion 15, 191 (1975)
[4] R. Schrittwieser, Phys. Lett. 65A, 235, (1978)
[5] P. Michelsen, H.L. Pécselli and J. Juul Rasmussen, Phys. Fluids 20, 866 (1977).
[6] P. Michelsen, RISO-R-417, National Laboratory, DK-4000 Roskilde, Denmark (1980)
[7] O. Ishihara and A. Hirose, Phys. Fluids, 27, 364 (1984)
[8] C.J. Pawley, H.E.Huey and N.C.Luhmann, Jr. Phys.Rev.Lett. 49, 877 (1982)
[9] H.S.W. Massey, E.H.S. Burkop and H.B. Gilbody, Electronic and Ionic Impact Phenomena, Oxford at the Clarendon Press, Vol. IV (1974)
[10] B.A. Al'terkop and A.A.Rukhadze, Sov. Phys.-JETP 35, 522 (1972).
[11] B.A. Al'terkop, Sov. Phys.-JETP 35, 915 (1972)
[12] E. Abu-Asali, B.A.Al'terkop and A.A.Rukhadze, Plasma Physics 17, 189 (1975)
[13] J.D. Swift, Ph.D.,B.Sc., F. INST.P. and M.J.R. Schwar, M.Sc., A. INST.P., London ILIFFE Books LTD (1970)
[14] H. Schneider and J. Szubert, Rev. Sci. Instrum. 48, 468 (1976)
[15] N. Hesselmann, Digitale Signalverarbeitung, Vogel-Verlag (1983)
[16] Y.C. Kim and E.J. Powers, IEEE Transactions on Plasma Science, Vol. PS-7, 120 (1979)
[17] Y.T. Acton DT. Squire, Solving Equations with physical understanding, A. Hilgler 1985
[18] E. Coddington, N. Levinson, Theory of Ordinary Differential Equations, Mc Graw-Hill, (1955)